

Search for NMSSM Higgs bosons in the $h \rightarrow aa \rightarrow \mu\mu \mu\mu, \mu\mu \tau\tau$ channels using $p\bar{p}$ collisions at $\sqrt{s} = 1.96$ TeV

V.M. Abazov³⁷, B. Abbott⁷⁵, M. Abolins⁶⁵, B.S. Acharya³⁰, M. Adams⁵¹, T. Adams⁴⁹, E. Aguilo⁶, M. Ahsan⁵⁹, G.D. Alexeev³⁷, G. Alkhozov⁴¹, A. Alton^{64,a}, G. Alverson⁶³, G.A. Alves², L.S. Ancu³⁶, T. Andeen⁵³, M.S. Anzelc⁵³, M. Aoki⁵⁰, Y. Arnoud¹⁴, M. Arov⁶⁰, M. Arthaud¹⁸, A. Askew^{49,b}, B. Åsman⁴², O. Atramentov^{49,b}, C. Avila⁸, J. BackusMayes⁸², F. Badaud¹³, L. Bagby⁵⁰, B. Baldin⁵⁰, D.V. Bandurin⁵⁹, S. Banerjee³⁰, E. Barberis⁶³, A.-F. Barfuss¹⁵, P. Bargassa⁸⁰, P. Baringer⁵⁸, J. Barreto², J.F. Bartlett⁵⁰, U. Bassler¹⁸, D. Bauer⁴⁴, S. Beale⁶, A. Bean⁵⁸, M. Begalli³, M. Begel⁷³, C. Belanger-Champagne⁴², L. Bellantoni⁵⁰, A. Bellavance⁵⁰, J.A. Benitez⁶⁵, S.B. Beri²⁸, G. Bernardi¹⁷, R. Bernhard²³, I. Bertram⁴³, M. Besançon¹⁸, R. Beuselinck⁴⁴, V.A. Bezzubov⁴⁰, P.C. Bhat⁵⁰, V. Bhatnagar²⁸, G. Blazey⁵², S. Blessing⁴⁹, K. Bloom⁶⁷, A. Boehnlein⁵⁰, D. Boline⁶², T.A. Bolton⁵⁹, E.E. Boos³⁹, G. Borisso⁴³, T. Bose⁶², A. Brandt⁷⁸, R. Brock⁶⁵, G. Brooijmans⁷⁰, A. Bross⁵⁰, D. Brown¹⁹, X.B. Bu⁷, D. Buchholz⁵³, M. Buehler⁸¹, V. Buescher²², V. Bunichev³⁹, S. Burdin^{43,c}, T.H. Burnett⁸², C.P. Buszello⁴⁴, P. Calfayan²⁶, B. Calpas¹⁵, S. Calvet¹⁶, J. Cammin⁷¹, M.A. Carrasco-Lizarraga³⁴, E. Carrera⁴⁹, W. Carvalho³, B.C.K. Casey⁵⁰, H. Castilla-Valdez³⁴, S. Chakrabarti⁷², D. Chakraborty⁵², K.M. Chan⁵⁵, A. Chandra⁴⁸, E. Cheu⁴⁶, D.K. Cho⁶², S. Choi³³, B. Choudhary²⁹, T. Christoudias⁴⁴, S. Cihangir⁵⁰, D. Claes⁶⁷, J. Clutter⁵⁸, M. Cooke⁵⁰, W.E. Cooper⁵⁰, M. Corcoran⁸⁰, F. Couderc¹⁸, M.-C. Cousinou¹⁵, S. Crépe-Renaudin¹⁴, D. Cutts⁷⁷, M. Ćwiok³¹, A. Das⁴⁶, G. Davies⁴⁴, K. De⁷⁸, S.J. de Jong³⁶, E. De La Cruz-Burelo³⁴, K. DeVaughan⁶⁷, F. Déliot¹⁸, M. Demarteau⁵⁰, R. Demina⁷¹, D. Denisov⁵⁰, S.P. Denisov⁴⁰, S. Desai⁵⁰, H.T. Diehl⁵⁰, M. Diesburg⁵⁰, A. Dominguez⁶⁷, T. Dorland⁸², A. Dubey²⁹, L.V. Dudko³⁹, L. Duflot¹⁶, D. Duggan⁴⁹, A. Duperrin¹⁵, S. Dutt²⁸, A. Dyshkant⁵², M. Eads⁶⁷, D. Edmunds⁶⁵, J. Ellison⁴⁸, V.D. Elvira⁵⁰, Y. Enari⁷⁷, S. Eno⁶¹, M. Escalier¹⁵, H. Evans⁵⁴, A. Evdokimov⁷³, V.N. Evdokimov⁴⁰, G. Facini⁶³, A.V. Ferapontov⁵⁹, T. Ferbel^{61,71}, F. Fiedler²⁵, F. Filthaut³⁶, W. Fisher⁵⁰, H.E. Fisk⁵⁰, M. Fortner⁵², H. Fox⁴³, S. Fu⁵⁰, S. Fuess⁵⁰, T. Gadfort⁷⁰, C.F. Galea³⁶, A. Garcia-Bellido⁷¹, V. Gavrilov³⁸, P. Gay¹³, W. Geist¹⁹, W. Geng^{15,65}, C.E. Gerber⁵¹, Y. Gershtein^{49,b}, D. Gillberg⁶, G. Ginther^{50,71}, B. Gómez⁸, A. Goussiou⁸², P.D. Grannis⁷², S. Greder¹⁹, H. Greenlee⁵⁰, Z.D. Greenwood⁶⁰, E.M. Gregores⁴, G. Grenier²⁰, Ph. Gris¹³, J.-F. Grivaz¹⁶, A. Grohsjean¹⁸, S. Grünendahl⁵⁰, M.W. Grünewald³¹, F. Guo⁷², J. Guo⁷², G. Gutierrez⁵⁰, P. Gutierrez⁷⁵, A. Haas⁷⁰, P. Haefner²⁶, S. Hagopian⁴⁹, J. Haley⁶⁸, I. Hall⁶⁵, R.E. Hall⁴⁷, L. Han⁷, K. Harder⁴⁵, A. Harel⁷¹, J.M. Hauptman⁵⁷, J. Hays⁴⁴, T. Hebbeker²¹, D. Hedin⁵², J.G. Hegeman³⁵, A.P. Heinson⁴⁸, U. Heintz⁶², C. Hensel²⁴, I. Heredia-De La Cruz³⁴, K. Herner⁶⁴, G. Hesketh⁶³, M.D. Hildreth⁵⁵, R. Hirosky⁸¹, T. Hoang⁴⁹, J.D. Hobbs⁷², B. Hoeneisen¹², M. Hohlfeld²², S. Hossain⁷⁵, P. Houben³⁵, Y. Hu⁷², Z. Hubacek¹⁰, N. Huske¹⁷, V. Hynek¹⁰, I. Iashvili⁶⁹, R. Illingworth⁵⁰, A.S. Ito⁵⁰, S. Jabeen⁶², M. Jaffré¹⁶, S. Jain⁷⁵, K. Jakobs²³, D. Jamin¹⁵, R. Jesik⁴⁴, K. Johns⁴⁶, C. Johnson⁷⁰, M. Johnson⁵⁰, D. Johnston⁶⁷, A. Jonckheere⁵⁰, P. Jonsson⁴⁴, A. Juste⁵⁰, E. Kajfasz¹⁵, D. Karmanov³⁹, P.A. Kasper⁵⁰, I. Katsanos⁶⁷, V. Kaushik⁷⁸, R. Kehoe⁷⁹, S. Kermiche¹⁵, N. Khalatyan⁵⁰, A. Khanov⁷⁶, A. Kharchilava⁶⁹, Y.N. Kharzhev³⁷, D. Khatidze⁷⁰, T.J. Kim³², M.H. Kirby⁵³, M. Kirsch²¹, B. Klima⁵⁰, J.M. Kohli²⁸, J.-P. Konrath²³, A.V. Kozelov⁴⁰, J. Kraus⁶⁵, T. Kuhl²⁵, A. Kumar⁶⁹, A. Kupco¹¹, T. Kurča²⁰, V.A. Kuzmin³⁹, J. Kvita⁹, F. Lacroix¹³, D. Lam⁵⁵, S. Lammers⁵⁴, G. Landsberg⁷⁷, P. Lebrun²⁰, W.M. Lee⁵⁰, A. Leflat³⁹, J. Lellouch¹⁷, J. Li^{78,†}, L. Li⁴⁸, Q.Z. Li⁵⁰, S.M. Lietti⁵, J.K. Lim³², D. Lincoln⁵⁰, J. Linnemann⁶⁵, V.V. Lipaev⁴⁰, R. Lipton⁵⁰, Y. Liu⁷, Z. Liu⁶, A. Lobodenko⁴¹, M. Lokajicek¹¹, P. Love⁴³, H.J. Lubatti⁸², R. Luna-Garcia^{34,d}, A.L. Lyon⁵⁰, A.K.A. Maciel², D. Mackin⁸⁰, P. Mättig²⁷, R. Magaña-Villalba³⁴, A. Magerkurth⁶⁴, P.K. Mal⁴⁶, H.B. Malbouisson³, S. Malik⁶⁷, V.L. Malyshev³⁷, Y. Maravin⁵⁹, B. Martin¹⁴, R. McCarthy⁷², C.L. McGivern⁵⁸, M.M. Meijer³⁶, A. Melnitchouk⁶⁶, L. Mendoza⁸, D. Menezes⁵², P.G. Mercadante⁵, M. Merkin³⁹, K.W. Merritt⁵⁰, A. Meyer²¹, J. Meyer²⁴, J. Mitrevski⁷⁰, N.K. Mondal³⁰, R.W. Moore⁶, T. Moulik⁵⁸, G.S. Muanza¹⁵, M. Mulhearn⁷⁰, O. Mundal²², L. Mundim³, E. Nagy¹⁵, M. Naimuddin⁵⁰, M. Narain⁷⁷, H.A. Neal⁶⁴, J.P. Negret⁸, P. Neustroev⁴¹, H. Nilsen²³, H. Nogima³, S.F. Novaes⁵, T. Nunnemann²⁶, G. Obrant⁴¹, C. Ochando¹⁶, D. Onoprienko⁵⁹, J. Orduna³⁴, N. Oshima⁵⁰, N. Osman⁴⁴, J. Osta⁵⁵, R. Otec¹⁰, G.J. Otero y Garzón¹, M. Owen⁴⁵, M. Padilla⁴⁸, P. Padley⁸⁰, M. Pangilinan⁷⁷, N. Parashar⁵⁶, S.-J. Park²⁴, S.K. Park³², J. Parsons⁷⁰, R. Partridge⁷⁷, N. Parua⁵⁴, A. Patwa⁷³, G. Pawloski⁸⁰, B. Penning²³, M. Perfilov³⁹, K. Peters⁴⁵, Y. Peters⁴⁵, P. Pétroff¹⁶, R. Piegaia¹, J. Piper⁶⁵, M.-A. Pleier²², P.L.M. Podesta-Lerma^{34,e}, V.M. Podstavkov⁵⁰, Y. Pogorelov⁵⁵, M.-E. Pol², P. Polozov³⁸, A.V. Popov⁴⁰, W.L. Prado da Silva³, S. Protopopescu⁷³, J. Qian⁶⁴, A. Quadt²⁴, B. Quinn⁶⁶, A. Rakitine⁴³,

M.S. Rangel¹⁶, K. Ranjan²⁹, P.N. Ratoff⁴³, P. Renkel⁷⁹, P. Rich⁴⁵, M. Rijssenbeek⁷², I. Ripp-Baudot¹⁹, F. Rizatdinova⁷⁶, S. Robinson⁴⁴, M. Rominsky⁷⁵, C. Royon¹⁸, P. Rubinov⁵⁰, R. Ruchti⁵⁵, G. Safronov³⁸, G. Sajot¹⁴, A. Sánchez-Hernández³⁴, M.P. Sanders²⁶, B. Sanghi⁵⁰, G. Savage⁵⁰, L. Sawyer⁶⁰, T. Scanlon⁴⁴, D. Schaile²⁶, R.D. Schamberger⁷², Y. Scheglov⁴¹, H. Schellman⁵³, T. Schliephake²⁷, S. Schlobohm⁸², C. Schwanenberger⁴⁵, R. Schwienhorst⁶⁵, J. Sekaric⁴⁹, H. Severini⁷⁵, E. Shabalina²⁴, M. Shamim⁵⁹, V. Shary¹⁸, A.A. Shchukin⁴⁰, R.K. Shivpuri²⁹, V. Siccaldi¹⁹, V. Simak¹⁰, V. Sirotenko⁵⁰, P. Skubic⁷⁵, P. Slattery⁷¹, D. Smirnov⁵⁵, G.R. Snow⁶⁷, J. Snow⁷⁴, S. Snyder⁷³, S. Söldner-Rembold⁴⁵, L. Sonnenschein²¹, A. Sopczak⁴³, M. Sosebee⁷⁸, K. Soustruznik⁹, B. Spurlock⁷⁸, J. Stark¹⁴, V. Stolin³⁸, D.A. Stoyanova⁴⁰, J. Strandberg⁶⁴, M.A. Strang⁶⁹, E. Strauss⁷², M. Strauss⁷⁵, R. Ströhmer²⁶, D. Strom⁵³, L. Stutte⁵⁰, S. Sumowidagdo⁴⁹, P. Svoisky³⁶, M. Takahashi⁴⁵, A. Tanasijczuk¹, W. Taylor⁶, B. Tiller²⁶, M. Titov¹⁸, V.V. Tokmenin³⁷, I. Torchiani²³, D. Tsybychev⁷², B. Tuchming¹⁸, C. Tully⁶⁸, P.M. Tuts⁷⁰, R. Unalan⁶⁵, L. Uvarov⁴¹, S. Uvarov⁴¹, S. Uzunyan⁵², P.J. van den Berg³⁵, R. Van Kooten⁵⁴, W.M. van Leeuwen³⁵, N. Varelas⁵¹, E.W. Varnes⁴⁶, I.A. Vasilyev⁴⁰, P. Verdier²⁰, L.S. Vertogradov³⁷, M. Verzocchi⁵⁰, D. Vilanova¹⁸, P. Vint⁴⁴, P. Vokac¹⁰, M. Voutilainen^{67,f}, R. Wagner⁶⁸, H.D. Wahl⁴⁹, M.H.L.S. Wang⁷¹, J. Warchol⁵⁵, G. Watts⁸², M. Wayne⁵⁵, G. Weber²⁵, M. Weber^{50,g}, L. Welty-Rieger⁵⁴, A. Wenger^{23,h}, M. Wetstein⁶¹, A. White⁷⁸, D. Wicke²⁵, M.R.J. Williams⁴³, G.W. Wilson⁵⁸, S.J. Wimpenny⁴⁸, M. Wobisch⁶⁰, D.R. Wood⁶³, T.R. Wyatt⁴⁵, Y. Xie⁷⁷, C. Xu⁶⁴, S. Yacoub⁵³, R. Yamada⁵⁰, W.-C. Yang⁴⁵, T. Yasuda⁵⁰, Y.A. Yatsunenko³⁷, Z. Ye⁵⁰, H. Yin⁷, K. Yip⁷³, H.D. Yoo⁷⁷, S.W. Youn⁵³, J. Yu⁷⁸, C. Zeitnitz²⁷, S. Zelitch⁸¹, T. Zhao⁸², B. Zhou⁶⁴, J. Zhu⁷², M. Zielinski⁷¹, D. Zieminska⁵⁴, L. Zivkovic⁷⁰, V. Zutshi⁵², and E.G. Zverev³⁹

(The DØ Collaboration)

¹Universidad de Buenos Aires, Buenos Aires, Argentina

²LAFEX, Centro Brasileiro de Pesquisas Físicas, Rio de Janeiro, Brazil

³Universidade do Estado do Rio de Janeiro, Rio de Janeiro, Brazil

⁴Universidade Federal do ABC, Santo André, Brazil

⁵Instituto de Física Teórica, Universidade Estadual Paulista, São Paulo, Brazil

⁶University of Alberta, Edmonton, Alberta, Canada; Simon Fraser University, Burnaby, British Columbia, Canada; York University, Toronto, Ontario, Canada and McGill University, Montreal, Quebec, Canada

⁷University of Science and Technology of China, Hefei, People's Republic of China

⁸Universidad de los Andes, Bogotá, Colombia

⁹Center for Particle Physics, Charles University,

Faculty of Mathematics and Physics, Prague, Czech Republic

¹⁰Czech Technical University in Prague, Prague, Czech Republic

¹¹Center for Particle Physics, Institute of Physics, Academy of Sciences of the Czech Republic, Prague, Czech Republic

¹²Universidad San Francisco de Quito, Quito, Ecuador

¹³LPC, Université Blaise Pascal, CNRS/IN2P3, Clermont, France

¹⁴LPSC, Université Joseph Fourier Grenoble 1, CNRS/IN2P3,

Institut National Polytechnique de Grenoble, Grenoble, France

¹⁵CPPM, Aix-Marseille Université, CNRS/IN2P3, Marseille, France

¹⁶LAL, Université Paris-Sud, IN2P3/CNRS, Orsay, France

¹⁷LPNHE, IN2P3/CNRS, Universités Paris VI and VII, Paris, France

¹⁸CEA, Irfu, SPP, Saclay, France

¹⁹IPHC, Université de Strasbourg, CNRS/IN2P3, Strasbourg, France

²⁰IPNL, Université Lyon 1, CNRS/IN2P3, Villeurbanne, France and Université de Lyon, Lyon, France

²¹III. Physikalisches Institut A, RWTH Aachen University, Aachen, Germany

²²Physikalisches Institut, Universität Bonn, Bonn, Germany

²³Physikalisches Institut, Universität Freiburg, Freiburg, Germany

²⁴II. Physikalisches Institut, Georg-August-Universität Göttingen, Göttingen, Germany

²⁵Institut für Physik, Universität Mainz, Mainz, Germany

²⁶Ludwig-Maximilians-Universität München, München, Germany

²⁷Fachbereich Physik, University of Wuppertal, Wuppertal, Germany

²⁸Panjab University, Chandigarh, India

²⁹Delhi University, Delhi, India

³⁰Tata Institute of Fundamental Research, Mumbai, India

³¹University College Dublin, Dublin, Ireland

³²Korea Detector Laboratory, Korea University, Seoul, Korea

³³SungKyunKwan University, Suwon, Korea

³⁴CINVESTAV, Mexico City, Mexico

- ³⁵FOM-Institute NIKHEF and University of Amsterdam/NIKHEF, Amsterdam, The Netherlands
³⁶Radboud University Nijmegen/NIKHEF, Nijmegen, The Netherlands
³⁷Joint Institute for Nuclear Research, Dubna, Russia
³⁸Institute for Theoretical and Experimental Physics, Moscow, Russia
³⁹Moscow State University, Moscow, Russia
⁴⁰Institute for High Energy Physics, Protvino, Russia
⁴¹Petersburg Nuclear Physics Institute, St. Petersburg, Russia
⁴²Stockholm University, Stockholm, Sweden, and Uppsala University, Uppsala, Sweden
⁴³Lancaster University, Lancaster, United Kingdom
⁴⁴Imperial College, London, United Kingdom
⁴⁵University of Manchester, Manchester, United Kingdom
⁴⁶University of Arizona, Tucson, Arizona 85721, USA
⁴⁷California State University, Fresno, California 93740, USA
⁴⁸University of California, Riverside, California 92521, USA
⁴⁹Florida State University, Tallahassee, Florida 32306, USA
⁵⁰Fermi National Accelerator Laboratory, Batavia, Illinois 60510, USA
⁵¹University of Illinois at Chicago, Chicago, Illinois 60607, USA
⁵²Northern Illinois University, DeKalb, Illinois 60115, USA
⁵³Northwestern University, Evanston, Illinois 60208, USA
⁵⁴Indiana University, Bloomington, Indiana 47405, USA
⁵⁵University of Notre Dame, Notre Dame, Indiana 46556, USA
⁵⁶Purdue University Calumet, Hammond, Indiana 46323, USA
⁵⁷Iowa State University, Ames, Iowa 50011, USA
⁵⁸University of Kansas, Lawrence, Kansas 66045, USA
⁵⁹Kansas State University, Manhattan, Kansas 66506, USA
⁶⁰Louisiana Tech University, Ruston, Louisiana 71272, USA
⁶¹University of Maryland, College Park, Maryland 20742, USA
⁶²Boston University, Boston, Massachusetts 02215, USA
⁶³Northeastern University, Boston, Massachusetts 02115, USA
⁶⁴University of Michigan, Ann Arbor, Michigan 48109, USA
⁶⁵Michigan State University, East Lansing, Michigan 48824, USA
⁶⁶University of Mississippi, University, Mississippi 38677, USA
⁶⁷University of Nebraska, Lincoln, Nebraska 68588, USA
⁶⁸Princeton University, Princeton, New Jersey 08544, USA
⁶⁹State University of New York, Buffalo, New York 14260, USA
⁷⁰Columbia University, New York, New York 10027, USA
⁷¹University of Rochester, Rochester, New York 14627, USA
⁷²State University of New York, Stony Brook, New York 11794, USA
⁷³Brookhaven National Laboratory, Upton, New York 11973, USA
⁷⁴Langston University, Langston, Oklahoma 73050, USA
⁷⁵University of Oklahoma, Norman, Oklahoma 73019, USA
⁷⁶Oklahoma State University, Stillwater, Oklahoma 74078, USA
⁷⁷Brown University, Providence, Rhode Island 02912, USA
⁷⁸University of Texas, Arlington, Texas 76019, USA
⁷⁹Southern Methodist University, Dallas, Texas 75275, USA
⁸⁰Rice University, Houston, Texas 77005, USA
⁸¹University of Virginia, Charlottesville, Virginia 22901, USA and
⁸²University of Washington, Seattle, Washington 98195, USA
(Dated: May 19, 2009)

We report on a first search for production of the lightest neutral CP-even Higgs boson (h) in the next-to-minimal supersymmetric standard model, where h decays to a pair of neutral pseudoscalar Higgs bosons (a), using 4.2 fb^{-1} of data recorded with the D0 detector at Fermilab. The a bosons are required to either both decay to $\mu^+\mu^-$ or one to $\mu^+\mu^-$ and the other to $\tau^+\tau^-$. No significant signal is observed, and we set limits on its production as functions of M_a and M_h .

PACS numbers: 12.60.Fr, 14.80.Cp

The CERN e^+e^- Collider (LEP) has excluded a SM-like Higgs boson decaying to $b\bar{b}$, $\tau^+\tau^-$ with a mass below 114.4 GeV [1], resulting in fine-tuning being needed in the minimal supersymmetric SM (MSSM). Slightly richer models, such as the next-to-MSSM (NMSSM) [2], allevi-

ate this fine-tuning [3]. The $h \rightarrow b\bar{b}$ branching ratio (BR) is greatly reduced because the h dominantly decays to a pair of lighter neutral pseudoscalar Higgs bosons (a). The most general LEP search yields $M_h > 82 \text{ GeV}$ [4], independent of the Higgs boson decay.

Helicity suppression causes the a boson to decay to the heaviest pair of particles kinematically allowed. The $\text{BR}(a \rightarrow \mu\mu)$ is nearly 100% for $2m_\mu < M_a \lesssim 3m_\pi$ (≈ 450 MeV) and then decreases with rising M_a due to decay into hadronic states [5]. A $M(\mu\mu)$ spectrum in Σ decays consistent with $a \rightarrow \mu\mu$ where $M_a = 214.3$ MeV was reported by the HyperCP collaboration [6], which suggests searching for $h \rightarrow aa$ with $a \rightarrow \mu\mu$ [7]. Decays to charm are usually suppressed in the NMSSM, so they have been neglected. If $2m_\tau < M_a < 2m_b$, the $\text{BR}(a \rightarrow \mu\mu)$ is suppressed by $(M_\mu^2/M_\tau^2)/[\sqrt{1 - (2M_\tau/M_a)^2}]$, a decays primarily to $\tau^+\tau^-$, and the limit from LEP is still weak ($M_h > 86$ GeV) [8]. The direct search for the 4τ final state is challenging, due to the lack of an observable resonance peak and low e, μ transverse momentum (p_T) which complicates triggering [9]. The $2\mu 2\tau$ final state however, contains a resonance from $a \rightarrow \mu\mu$, high p_T muons for triggering, and missing transverse energy (\cancel{E}_T) [10]. B-factories also search for $\Upsilon \rightarrow a\gamma$, where the a boson escapes as missing energy or decays to muons or taus [11].

In this Letter, we present a first search for h boson production, followed by $h \rightarrow aa$ decay with either both a bosons decaying to $\mu^+\mu^-$ or one decaying to $\mu^+\mu^-$ and the other to $\tau^+\tau^-$. Data from Run II of the Fermilab Tevatron Collider recorded with the D0 detector [12] are used, corresponding to an integrated luminosity of about 4.2 fb^{-1} . The signal signature is either two pairs of collinear muons (due to the low M_a), or one pair of collinear muons and either large \cancel{E}_T , an additional (not necessarily isolated) muon, or a loosely-isolated electron from $a \rightarrow \tau\tau$ opposite to the muon pair. The main backgrounds are multijet events containing muons from the decay of particles in flight (π, K), heavy-flavor decays, and other sources ($\eta, \phi, J/\psi$, etc.) and $Z/\gamma^*(\rightarrow \mu\mu) + \text{jets}$. The PYTHIA [13] event generator is used to simulate $gg \rightarrow h \rightarrow aa$ signal events for various M_h and M_a , which are then passed through the GEANT3 [14] D0 detector simulation and reconstructed.

Events are required to have at least two muons reconstructed in the muon system and matched to tracks from the inner tracking system with $p_T > 10$ GeV and $|\eta| < 2$, where η is the pseudorapidity. Muons are not required to have opposite electric charge. No specific trigger requirements are made; an OR of all implemented triggers is used. But most events selected pass a dimuon trigger, with muon p_T thresholds of 4–6 GeV. Trigger efficiency is $>90\%$ for events passing the offline selections.

For the 4μ channel, we look for one muon from each of the two a boson decays, so the dimuon pair with the largest invariant mass is selected, with $M(\mu, \mu) > 15$ GeV and $\Delta\mathcal{R}(\mu, \mu) > 1$, where $\Delta\mathcal{R} = \sqrt{(\Delta\eta)^2 + (\Delta\phi)^2}$ and ϕ is the azimuthal angle. Only one muon is required to be reconstructed from each pair of collinear muons. The muon system has insufficient granularity to reliably reconstruct two close muons. A companion track is identified with $p_T > 4$ GeV and smallest $\Delta\mathcal{R}$ from each muon, within

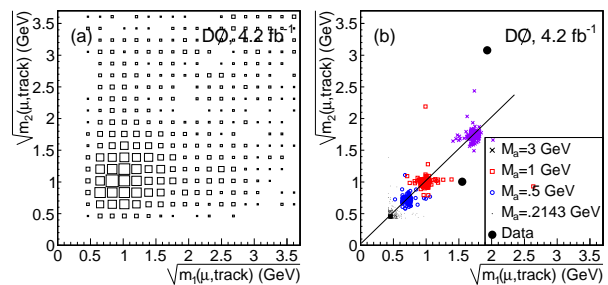


FIG. 1: The $\sqrt{m_2(\mu, \text{track})}$ vs. $\sqrt{m_1(\mu, \text{track})}$ distribution (a) in the multijet sample, and (b) after the isolation cut is applied to both muons for data and various MC signal masses.

$\Delta\mathcal{R} < 1$ and $\Delta z(\text{track}, \text{PV}) < 1$ cm, where z is the distance along the beamline, and PV is the primary $p\bar{p}$ interaction vertex. The muon pair calorimeter isolation ($\mathcal{I}_{\mu\mu}^C$) is the sum of calorimeter energy within $0.1 < \Delta\mathcal{R} < 0.4$ of either the muon or the companion track. Both muons are required to have $\mathcal{I}_{\mu\mu}^C < 1$ GeV and track-based isolation: ≤ 3 tracks with $p_T > 0.5$ GeV and $\Delta z(\text{track}, \text{PV}) < 1$ cm within $\Delta\mathcal{R} < 0.5$ of the muon, including the muon track itself.

Based on a control data sample greatly enhanced in multijet events by removing the $\mathcal{I}_{\mu\mu}^C$ requirement on the muons, we predict 1.9 ± 0.4 events to pass the final selections. The mass of the leading (trailing) p_T muon and its companion track, $m_1(\mu, \text{track})$ ($m_2(\mu, \text{track})$), is shown in the multijet sample in Fig. 1(a) and is used to model the background shape. Background is also expected from $Z/\gamma^* \rightarrow \mu\mu$ events where additional companion tracks are reconstructed. Studying the dimuon mass distributions in the isolated data when zero or one of the muons is required to have a companion track gives an estimate of 0.29 ± 0.04 events. The background from $t\bar{t}$, diboson, and $W + \text{jets}$ production is found to be negligible.

Signal acceptance uncertainty is dominated by the ability to simulate the detection of the companion track, particularly when the two muons are very collinear. We compare K_S^0 decays in data and simulation as a function of the $\Delta\mathcal{R}$ between the two pion tracks. Over most of the $\Delta\mathcal{R}$ range, the relative tracking efficiency is within 20%, but few events have $\Delta\mathcal{R} < 0.02$ (corresponding to $M_a < 0.5$ GeV for $M_h = 100$ GeV), and consistency can only be confirmed at the 50% level. For $\Delta\mathcal{R}(\mu, \mu) < 0.1$ (corresponding to $M_a < 2$ GeV for $M_h = 100$ GeV), there is the possibility that the two muons will overlap in the muon system and interfere with each other's proper reconstruction and triggering. By studying the effect of adding noise hits, we find up to a 10% effect on reconstruction and 20% effect on the trigger efficiency. The background uncertainty (50%) is dominated by the statistical uncertainty of the multijet-enhanced data sample. The luminosity uncertainty is 6.1% [15].

After the isolation requirements are applied to both muons, two events are observed in data, consistent with

TABLE I: The efficiency for MC signal events within the 2 s.d. window around each M_a , numbers of events expected from background (with statistical uncertainty) and observed in data, and the expected and observed limits on the $\sigma(p\bar{p}\rightarrow h+X)\times\text{BR}(h\rightarrow aa\rightarrow 4\mu)$, for $M_h=100$ GeV. Limits for other M_a , up to $2m_\tau$, are interpolated from these simulated MC samples. No events are observed in a window for any interpolated M_a .

M_a (GeV)	Window (MeV)	Eff.	N_{bckg}	N_{obs}	$\sigma\times\text{BR}$ [exp] obs (fb)
0.2143	± 15	17%	0.001 ± 0.001	0	[10.0] 10.0
0.3	± 50	16%	0.006 ± 0.002	0	[9.5] 9.5
0.5	± 70	12%	0.012 ± 0.004	0	[7.3] 7.3
1	± 100	13%	0.022 ± 0.005	0	[6.1] 6.1
3	± 230	14%	0.005 ± 0.002	0	[5.6] 5.6

the total background of 2.2 ± 0.5 events. Neither has a third muon identified, compared to about 50% of the signal MC events. We fit a Gaussian distribution to the $m_1(\mu, \text{track})$ distribution, and the number of events with both $m_1(\mu, \text{track})$ and $m_2(\mu, \text{track})$ within a ± 2 s.d. window around the mean from the fit are determined for data, signal, and background (Tab. I). No events are observed within any window, in agreement with the background prediction. Upper limits on the $h\rightarrow aa\rightarrow 4\mu$ signal rate are computed at 95% C.L. using a Bayesian technique [16] and vary slightly with M_h , decreasing by $\approx 10\%$ when M_h increases from 80 to 150 GeV.

For the $2\mu 2\tau$ channel, the muon pair is selected in each event with the largest scalar sum of muon p_T ($\Sigma_\mu^{p_T}$), with muon $p_T > 10$ GeV, $\Delta\mathcal{R}(\mu, \mu) < 1$, and $M(\mu\mu) < 20$ GeV. This is the “pre-selection” (Tab. II). Next, $\Sigma_\mu^{p_T} > 35$ GeV is required, to reduce background, and the same muon pair calorimeter and track isolation cuts are applied as for the 4μ channel. This is the “isolated” selection.

Standard D0 τ identification [17] is severely degraded and complicated by the topology of the two overlapping τ leptons. Instead, we require significant \cancel{E}_T from the collinear τ decays to neutrinos. The \cancel{E}_T is computed from calorimeter cell energies and corrected for the p_T of the muons. To ensure that this correction is as accurate as possible, the following additional muon selection criteria are applied. The muons’ tracks in the inner tracker are required to have fits to their hits with $\chi^2/\text{dof} < 4$, transverse impact parameter from the PV less than 0.01 cm, and at least three hits in the silicon detector. The match between the track reconstructed from muon system hits and the track in the inner tracker must have $\chi^2 < 40$, and the muon system track must have $p_T > 8$ GeV. Hits are required for both muons in all three layers of the muon system. Also, less than 10 GeV of calorimeter energy is allowed within $\Delta\mathcal{R} < 0.1$ of either muon, to exclude muons with showers in the calorimeter. Finally, the leading muon p_T must be less than 80 GeV, to remove muons

with mismeasured p_T . To improve the \cancel{E}_T measurement in the calorimeter, the number of jets reconstructed [18] with cone radius 0.5, $p_T > 15$ GeV (corrected for jet energy scale), and $|\eta| < 2.5$ must be less than five. Events with $\cancel{E}_T > 80$ GeV are also rejected to remove rare events where the \cancel{E}_T is grossly mismeasured, since signal is not expected to have such large \cancel{E}_T . These are the “refining” cuts. Then an event must pass one of three mutually exclusive subselections. The first subselection, for when no jet is reconstructed from the tau pair, requires zero jets with $p_T > 15$ GeV, $\Delta\phi(\mu\mu, \cancel{E}_T) > 2.5$, the highest- p_T track with $\Delta z(\text{track}, \text{PV}) < 3$ cm and not matching either of the two selected muon tracks in the dimuon candidate to have $p_T > 4$ GeV and $\Delta\phi(\text{track}, \cancel{E}_T) < 0.7$. The second subselection, for when at least one of the tau decays is 1-prong, requires at least one jet, where the leading- p_T jet (jet1) has no more than four (non-muon) tracks associated with it with $p_T > 0.5$ GeV, $\Delta z(\text{track}, \text{jet1}) < 3$ cm, and $\Delta\mathcal{R}(\text{track}, \text{jet1}) < 0.5$, $\Delta\phi(\text{jet1}, \cancel{E}_T) < 0.7$, and $\cancel{E}_T > 20$ GeV. The third subselection, for when both tau decays are 3-prong (or more) and thus most jet-like, requires at least one jet, where jet1 has either more than four (non-muon) tracks associated with it or $\Delta\phi(\text{jet1}, \cancel{E}_T) > 0.7$ and $\cancel{E}_T > 35$ GeV. Events passing one of these three subselections are called the “ \cancel{E}_T ” selection.

To gain acceptance, we also select events not passing the “ \cancel{E}_T ” selection, but with either an additional muon (not necessarily isolated) or loosely-isolated electron. For the “Muon” selection, a (third) muon is required, with $p_T > 4$ GeV and $\Delta\phi(\mu, \cancel{E}_T) < 0.7$. The “EM” selection rejects events in the “Muon” selection and then requires an electron with $p_T > 4$ GeV, $\Delta\phi(e, \cancel{E}_T) < 0.7$, fewer than three jets, $\cancel{E}_T > 10$ GeV, and $p_T^e + \cancel{E}_T > 35$ GeV.

The dimuon invariant mass shape of the multijet and γ^* background to the “ \cancel{E}_T ” selection is estimated from the low \cancel{E}_T data which passes the “refining” cuts but fails the “ \cancel{E}_T ” selection cuts. For the “Muon” and “EM” selections, it is taken from the “isolated” data sample. The requirements of the “Muon” and “EM” selections have no significant effect on the dimuon invariant mass shape for a data sample with loosened isolation requirements. These background shapes are summed and normalized to the data passing all selections, but excluding data events within a 2 s.d. dimuon mass window for each M_a (see below). Background from diboson, $t\bar{t}$, and W +jets production, containing true \cancel{E}_T from neutrinos, is estimated using MC and found to contribute $< 10\%$ of the background from multijet and γ^* .

Signal acceptance uncertainty for the $2\mu 2\tau$ channel is dominated by the ability of the simulation to model the efficiency of the “refining” muon cuts and final selections. It is found to be 20% per-event based on studies of the muon and event quantities used, comparing data and MC events in the Z boson mass region. Comparing the J/ψ and Z boson yields gives a 10% trigger efficiency uncertainty. The background uncertainty is less than 20% and

TABLE II: Selection efficiencies and limits for the $2\mu 2\tau$ channel, for $M_h=100$ GeV and various M_a . The numbers of events at “pre-selected,” “isolated” stages and after (“refining”) “ \cancel{E}_T ,” “Muon,” and “EM” selections, assuming $\sigma(p\bar{p}\rightarrow h+X)=1.9$ pb and $\text{BR}(h\rightarrow aa)=1$. Next are the window size, and numbers of events in the window for signal (and overall efficiency times BR), expected from background (with statistical uncertainty), and observed in data. The expected and observed limits on $\sigma(p\bar{p}\rightarrow h+X)\times\text{BR}(h\rightarrow aa)$ and $\sigma(p\bar{p}\rightarrow h+X)\times\text{BR}(h\rightarrow aa)\times 2\times\text{BR}(a\rightarrow\mu\mu)\times\text{BR}(a\rightarrow\tau\tau)$ follow.

Sample	N pre.	N iso.	(ref.) “ \cancel{E}_T ”	“Mu”	“EM”	Window	N_{sig} (Eff.)	N_{bckg}	N_{obs}	[exp] obs	$\sigma\times 2\times\text{BR}$
Data	95793	2795	(1085) 15	4	4						
$M_a=3.6$ GeV	53.1	28.0	(14.5) 3.5	1.9	0.8	± 0.30 GeV	5.2 (0.066%)	1.9 ± 0.4	1	[1.8] 1.5 pb	[23.8] 19.1 fb
$M_a=4$ GeV	33.6	15.3	(8.1) 2.5	1.2	0.4	± 0.32 GeV	3.3 (0.042%)	1.1 ± 0.2	4	[2.6] 4.9 pb	[23.9] 45.9 fb
$M_a=7$ GeV	20.6	8.7	(4.5) 1.7	0.8	0.3	± 0.54 GeV	2.1 (0.027%)	1.1 ± 0.2	1	[4.0] 3.9 pb	[25.0] 24.6 fb
$M_a=10$ GeV	19.3	7.5	(4.2) 1.1	0.6	0.3	± 0.95 GeV	1.5 (0.020%)	1.6 ± 0.3	2	[5.9] 6.5 pb	[24.7] 27.3 fb
$M_a=19$ GeV	14.6	5.4	(2.9) 0.8	0.4	0.2	± 1.37 GeV	1.2 (0.015%)	0.6 ± 0.1	1	[6.3] 7.1 pb	[30.0] 33.7 fb

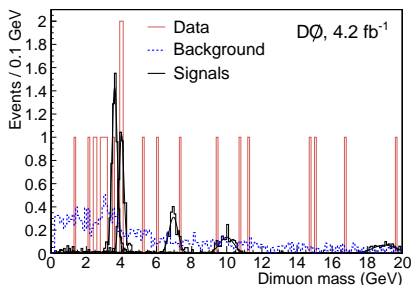


FIG. 2: The dimuon invariant mass for events passing all selections in data, background, and $2\mu 2\tau$ signals for $M_a = 3.6, 4, 7, 10,$ and 19 GeV. $\sigma(p\bar{p}\rightarrow h+X)=1.9$ pb is assumed, $\text{BR}(h\rightarrow aa)=1$, and $M_h=100$ GeV.

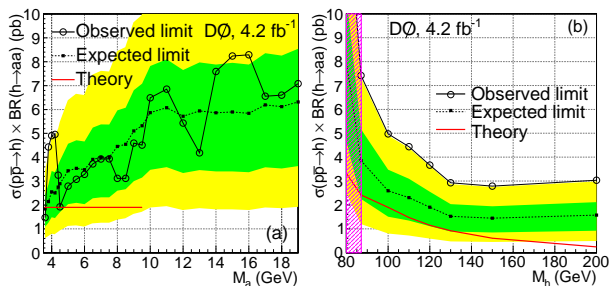


FIG. 3: The expected and observed limits and ± 1 s.d. and ± 2 s.d. expected limit bands for $\sigma(p\bar{p}\rightarrow h+X)\times\text{BR}(h\rightarrow aa)$, for (a) $M_h=100$ GeV and (b) $M_a=4$ GeV. The signal for $\text{BR}(h\rightarrow aa)=1$ is shown by the solid line. The region $M_h<86$ GeV is excluded by LEP.

dominated by the statistical uncertainty of the data sample used. Alternate fits of the background shape from low \cancel{E}_T data modify the background estimates by up to 10%.

Figure 2 shows the dimuon invariant mass for data, background, and signals, after all selections. Each signal dimuon mass peak is fit to a Gaussian distribution, and the numbers of events with dimuon mass within a ± 2 s.d. window around the mean from the fit are counted (Tab. II). Data in each window are consistent with the

predicted background. The expected and observed limits on the $\sigma\times\text{BR}$ of the $h\rightarrow aa$ process for each M_a studied are shown, assuming the a boson BRs given by PYTHIA, with no charm decays. Since the a boson BRs are model-dependent, we also derive a result which factors out the BRs taken from PYTHIA. Limits are derived for intermediate M_a by interpolating the signal efficiencies and window sizes, see Fig. 3(a). Above 9.5 GeV, we expect $a\rightarrow b\bar{b}$ decays to dominate and greatly decrease $\text{BR}(aa\rightarrow 2\mu 2\tau)$, but limits are calculated under the assumption that the b quark decays are absent. We also study the limits vs. M_h for $M_a = 4$ GeV, see Fig. 3(b).

We have presented results of the first search for Higgs boson production in the NMSSM decaying into a bosons at a high energy hadron collider, in the 4μ and $2\mu 2\tau$ channels. The predicted $\text{BR}(a\rightarrow\mu\mu)$ is driven at low M_a by competition between decays to $\mu\mu$ and to gluons and has large theoretical uncertainties [19]. Therefore, for $M_a<2m_\tau$, we set limits only on $\sigma(p\bar{p}\rightarrow h+X)\times\text{BR}(h\rightarrow aa)\times\text{BR}^2(a\rightarrow\mu^+\mu^-)$, excluding about 10 fb. Assuming $\sigma(p\bar{p}\rightarrow h+X)=1.9$ pb [20], corresponding to $M_h\approx 100$ GeV, $\text{BR}(a\rightarrow\mu\mu)$ must therefore be less than 7% to avoid detection, assuming a large $\text{BR}(h\rightarrow aa)$. However, $\text{BR}(a\rightarrow\mu\mu)$ is expected to be larger than 10% for $M_a<2m_c$ [5], and depending on $\text{BR}(a\rightarrow c\bar{c})$, which is model-dependent and typically suppressed in the NMSSM, could remain above 10% until $M_a=2m_\tau$. Thus these results severely constrain the region $2m_\mu<M_a<2m_\tau$. For $M_a>2m_\tau$, the limits set by the current analysis are a factor of $\approx 1-4$ larger than the expected production cross section.

We thank the staffs at Fermilab and collaborating institutions, and acknowledge support from the DOE and NSF (USA); CEA and CNRS/IN2P3 (France); FASI, Rosatom and RFBR (Russia); CNPq, FAPERJ, FAPESP and FUNDUNESP (Brazil); DAE and DST (India); Colciencias (Colombia); CONACyT (Mexico); KRF and KOSEF (Korea); CONICET and UBACyT (Argentina); FOM (The Netherlands); STFC and the Royal Society (United Kingdom); MSMT and GACR (Czech

Republic); CRC Program, CFI, NSERC and WestGrid Project (Canada); BMBF and DFG (Germany); SFI (Ireland); The Swedish Research Council (Sweden); CAS and CNSF (China); and the Alexander von Humboldt Foundation (Germany).

-
- [a] Visitor from Augustana College, Sioux Falls, SD, USA.
 [b] Visitor from Rutgers University, Piscataway, NJ, USA.
 [c] Visitor from The University of Liverpool, Liverpool, UK.
 [d] Visitor from Centro de Investigacion en Computacion - IPN, Mexico City, Mexico.
 [e] Visitor from ECFM, Universidad Autonoma de Sinaloa, Culiacán, Mexico.
 [f] Visitor from Helsinki Institute of Physics, Helsinki, Finland.
 [g] Visitor from Universität Bern, Bern, Switzerland.
 [h] Visitor from Universität Zürich, Zürich, Switzerland.
 [‡] Deceased.
- [1] R. Barate *et al.*, Phys. Lett. B **565**, 61 (2003).
 [2] U. Ellwanger, M. Rausch de Traubenberg, and C. A. Savoy, Nucl. Phys. **B492**, 21 (1997).
 [3] R. Dermisek and J.F. Gunion, Phys. Rev. Lett. **95**, 041801 (2005); S. Chang, R. Dermisek, J. F. Gunion, and N. Weiner, Ann. Rev. Nucl. Part. Sci. **58**, 75 (2008).
 [4] G. Abbiendi *et al.* (OPAL Collaboration), Eur. Phys. J. C **27**, 311 (2003).
 [5] K. Cheung, J. Song, P. Tseng, and Q. S. Yan, Phys. Rev.

- D **78**, 055015 (2008).
 [6] H. Park *et al.* (HyperCP Collaboration), Phys. Rev. Lett. **94**, 021801 (2005).
 [7] P. Yin and S. Zhu, arXiv:hep-ph/0611270 (2006).
 [8] S. Schael *et al.* (ALEPH Collaboration), Eur. Phys. J. C **47**, 547 (2006).
 [9] P. W. Graham, A. Pierce and J. G. Wacker, arXiv:hep-ph/0605162 (2006).
 [10] M. Lisanti and J. G. Wacker, arXiv:0903.1377 [hep-ph] (2009).
 [11] B. Aubert *et al.* (BaBar Collaboration), arXiv:0808.0017 [hep-ex] (2008); W. Love *et al.* (CLEO Collaboration), Phys. Rev. Lett. **101**, 151802 (2008); B. Aubert *et al.* (BaBar Collaboration), arXiv:0906.2219 [hep-ex] (2009).
 [12] V. Abazov *et al.* (D0 Collaboration), Nucl. Instrum. Methods Phys. Res. A **565**, 463 (2006).
 [13] T. Sjöstrand *et al.*, Comput. Phys. Commun. **135**, 238 (2001). [Version 6.323]
 [14] R. Brun and F. Carminati, CERN Program Library Long Wwriteup W5013, 1993 (unpublished).
 [15] T. Andeen *et al.*, FERMILAB-TM-2365 (2007).
 [16] I. Bertram *et al.*, FERMILAB-TM-2104 (2000).
 [17] V. Abazov *et al.* (D0 Collaboration), Phys. Lett. B **670**, 292 (2009).
 [18] G. C. Blazey *et al.*, arXiv:hep-ex/0005012 (2000).
 [19] Gunion J. F., “The Higgs Hunter’s Guide”, p.34-40, Perseus Publishing, 1990.
 [20] D. de Florian and M. Grazzini, arXiv:0901.2427v1 [hep-ph] (2009).